URSI GASS 2020, Rome, Italy, 29 August - 5 September 2020

mm-Wave Chipless RFID Tag for Healthcare Applications

Alessandro DiCarlofelice[(1)], Emidio DiGiampaolo[(1)], and Piero Tognolatti[(1)]
[(1)] Department of Industrial and Information Engineering and Economics, University of L'Aquila, Italy

Abstract

The work proposes the use of mm-wave chipless tag to be used in healthcare applications. A chipless tag at 24 GHz based on a cross-polarized Van Atta retrodirective array has been designed with the aim to show the practical feasibility of the proposed system. Numerical results of a small array made of 6 elements show a good RCS level that makes that kind of chipless tag promising for indoor healthcare monitoring.

1 Introduction

The increasing of the healthcare cost has become an issue of high priority for governments and healthcare organizations. It can be limited by the use of health information technology that improves the patient safety and the quality of care and may lead to additional savings researching for low-cost technology [1]. Radio Frequency Identification (RFID) technology offers a practical opportunity to face that issue since it gives means and methods for reducing errors in patient care, facilitating tracing and tracking of patients and equipment, and allowing better management of healthcare assets [2]. Furthermore, Ultrahigh frequency (UHF) RFID technology is currently investigated for extending its functionality to sensing applications, in particular, in the context of healthcare, for monitoring vital signs, such as heart rate, breathing, blood pressure, and sleep disorders like sleep apnea. A branch of evolution of that technology resorts to chipless tags that encode data in the frequency signature of the backscattered signal avoiding the use of a microchip to store the ID and perform sensing [3]. When a chipless tag is radiated with a frequency modulated continuous wave (FMCW) chirp that spans over a sufficiently wide bandwidth it performs a selective backscattering of the impinging chirp, i.e. the different frequency components of the chirp are backscattered with different amplitude and phase according to the characteristics of the frequency response of the tag. Clearly, if the tag has been designed to backscatter with a specific selective spectrum it is uniquely identified by its spectrogram. The unique ID spectrogram of a chipless tags is typically obtained using a wide or ultrawide band antenna loaded with a set of narrowband resonating circuits that produces notches in the frequency response and each resonant frequency (or notch) is considered as a bit of the ID [4, 5]. The main drawback of this kind of tags is the short reading range (typically in the order of tens of centimeters or less) because of the low Radar Cross Section (RCS) of the used antennas and the clutter from adjacent objects that camouflages the backscattered signal. Cross polarized tags exploit polarization diversity in order to improve the useful signal with respect to the clutter, they, in fact, backscatter a cross-polarized field while the clutter backscatter in co-polarization [6, 7]. Evidently, the increasing of RCS can be achieved with electrically big tag's antenna, but it is impractical at UHF band because the size of the antenna becomes incompatible with the small dimensions required for a tag. Nevertheless, the size of electrically large antenna can be taken physical small at mm-wave band where array of antennas having very high RCS appear well suited for this kind of applications. The detection range at this frequency band can be increased exploiting retrodirective arrays (e.g. Van Atta model) whose RCS is independent from the direction for a wide angular extension [8]. A further advantage of mm-wave band is the reuse of the low-cost automotive FMCW radar as reader of chipless tags [9]. In fact, automotive radar is suited for that application because it complies with both large bandwidth to encode data and effective methods to localize the tag and extract its ID and data sensor. Many off-the-shelf FMCW automotive radar are available to accomplish this goal at 24GHz and 79GHz bands allowing for a very low-cost RFID chipless system.

In this work we develop a chipless tag at 24 GHz for healthcare applications that is based on a cross-polarized Van Atta retrodirective array. The tag is based on microstrip patch antennas fed by slots over the ground plane of a stripline network configured for retrodirective mode. The feeding network includes coupled narrowband resonators that codify the spectral signature of the tag. The ground plane of the stripline allows a complete decoupling of the tag from the body where it is placed on and preserves the tag from interference. The paper is organized as follows: Section 2 shows the basic requirements for the system, Section 3 concerns the description of the tag while Section 4 reports numerical results.

2 System requirements

For the sake of simplicity, we conceive the basic system consisting of an off-the-shelf automotive radar and a tag. The reuse of the frequency band of automotive radar at 24 GHz allows a bandwidth of about 2 GHz sufficiently large for encoding some bits. The maximum theoretical distance between radar and tag antennas that permits the detection of the tag can be estimated by means of the monostatic radar equation:

$$R_{max} = \sqrt[4]{\frac{P_t G^2 \lambda^2 \sigma}{P_{r\,min}(4\pi)^3 L_{loss}}} \quad (1)$$

where P_t is the transmitted power, G is the radar's antenna gain, λ is the wavelength, σ is the tag's RCS, $P_{r\,min}$ is the smallest received power that can be detect by the radar and L_{loss} is a factor accounting for all possible losses. Considering the ideal lossless case and that an off-the-shelf automotive radar may have an output power of about *8 dBm* and a receiver sensibility of about *-100 dBm* the maximum detection distance for an antenna's gain of 5 dB is larger than 2 m even for very small RCS as shown in Fig. 1. Such a distance makes chipless tags promising for short range applications.

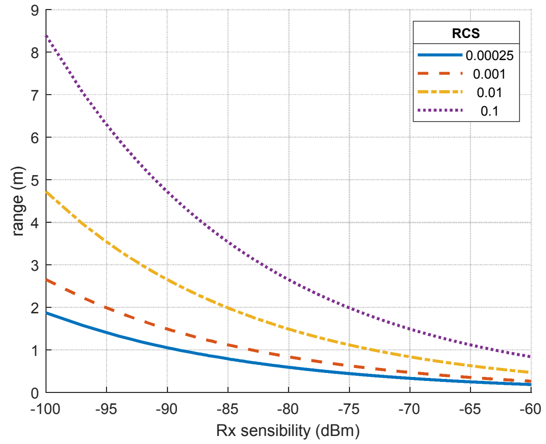

Figure 1. Losseless radar range @ 24 GHz vs. receiver sensibility for different values of tag's RCS, 8 dBm transmitting power with 5 dB antenna's gain.

3 Tag description

The three-dimensional structure of the proposed tag antenna is shown in Fig. 2 where the dielectric parts are removed. It consists of two sets of 3 rectangular patches, a set is deployed on the positive part of *x* axis while the other is in the negative part. The two sets are distinguished by different (orthogonal) polarization. The patches are fed by slots (pale yellow strips) made on the ground plane (not shown) of a stripline network. The network consists of lines of equal length that feed slots of patches belonging to different set. That topology realizes a retro-directive Van Atta array that retro-reflects the imping signal in the orthogonal polarization. The network includes some U-shaped resonators (three in the present model) that are used for spectral signature and sensing and stubs for matching lines to slots. The stripline has been designed on RT/Duroid 5880 that has relative permittivity *2.2*, tangent of loss angle *0.001* and thickness *0.508 mm*. Patches lie on a substrate having thickness *1.4 mm* and relative permittivity *1.1*. The overall dimensions of the tag are about $60 \times 20 \times 2\ mm^3$ resulting similar to that of a UHF RFID tag.

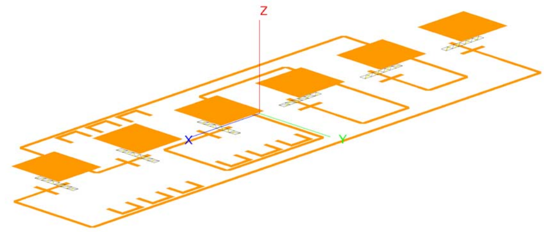

Figure 2. 3D layout of the tag antenna with dielectric layers and ground planes removed. The visible parts are: patches, slots and network that lie on three different layers. U-shaped resonators are also visible.

4 Numerical results

The tag model has been analyzed with Method of Moment based simulation tool (*Altair Feko* [10]) over the frequency interval between 23 and 27 GHz and for a plane wave impinging from different angles. Figure 3 shows the obtained RCS of the crosspolar component over the cutting plane parallel to the array deployment and for three different impinging angles: 0°, 15° and 30°. The retrodirective lobes are clearly obtained with a level greater than -35dB. That RCS level permits a detection distance of about 2 m as shown in Fig.1. Figure 4 shows the crosspolar RCS vs. frequency, the spectral signature impressed by the three resonators is shown by the three clear notches. The position of the notches does not change with the impinging angle while their depth remains sufficiently long to be easily distinguished. An additional FDTD model of the tag over a human forearm, shown in Fig. 5, has confirmed the achieved results.

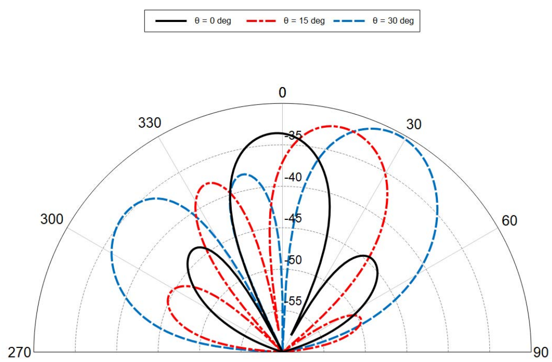

Figure 3. Cross-polar RCS diagrams of the tag @ 25 GHz and for plane waves impinging from three different angles: 0° (continuous black), 15° (dash-dotted red), 30° (dashed blue).

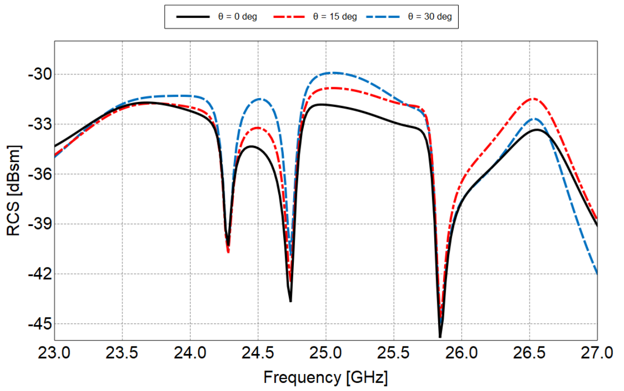

Figure 4. Monostatic cross-polar RCS of the tag vs. frequency for plane waves impinging from three different angles: 0° (continuous black), 15° (dash-dotted red), 30° (dashed blue). The spectral signature is clearly shown by three notches within the 24-26 GHz band.

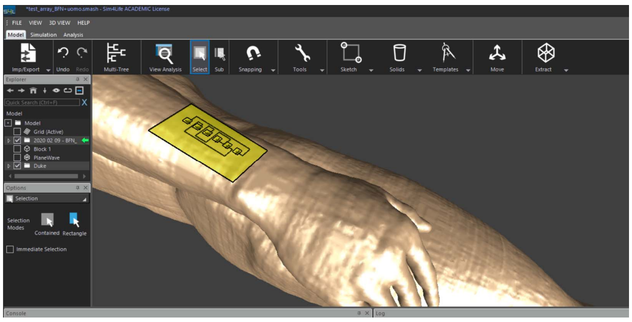

Figure 5. FDTD model of the proposed chipless tag, when positioned on a portion of a human forearm. Analyzed by *Sim4Life* simulation platform [11].

5 Conclusion

The obtained results show the possibility to develop small chipless tag at mm-wave frequency band to be used in healthcare applications for both the identification of people and objects and the remote monitoring of the health status of patients. Exploiting the cross-polarized Van Atta retrodirective array it is possible to obtain RCS levels sufficiently high to detect the tag from few meters. The designed tag encodes only three bits but more bits are possible with an optimization of the use of the bandwidth. A next experimental activity will check the obtained results.

6 References

1. B. Farahani, F. Firouzi, K. Chakrabarty, *Healthcare IoT*, In: Firouzi F., Chakrabarty K., Nassif S. (eds) Intelligent Internet of Things. Springer, Cham, 2020.

2. J. E. Camacho-Cogollo, I. Bonet, E. Iadanzac, *RFID technology in health care*, In: Clinical Engineering Handbook (Second Edition), 2020, pp. 33-41, doi: B978-0-12-813467-2.00004-3.

3. T. Athauda and N. Karmakar, "Chipped Versus Chipless RF Identification: A Comprehensive Review," *IEEE Microwave Magazine*, **20**, 9, Sept. 2019, pp. 47-57, doi: 10.1109/MMM.2019.2922118.

4. M. A. Islam and N. Karmakar, "Compact printable chipless RFID tags using polarization diversity," 42nd European Microwave Conference, Amsterdam, 2012, pp. 912-915, doi: 10.23919/EuMC.2012.6459088.

5. M. Khaliel, A. El-Awamry, A. Fawky, M. El-Hadidy and T. Kaiser, "A novel co/cross-polarizing chipless RFID tags for high coding capacity and robust detection," IEEE International Symposium on Antennas and Propagation & USNC/URSI National Radio Science Meeting, Vancouver, BC, 2015, pp. 159-160, doi: 10.1109/APS.2015.7304465.

6. A. Vena, E. Perret and S. Tedjni, "A Depolarizing Chipless RFID Tag for Robust Detection and Its FCC Compliant UWB Reading System," *IEEE Transactions on Microwave Theory and Techniques*, **61**, 8, Aug. 2013, pp. 2982-2994, doi: 10.1109/TMTT.2013.2267748.

7. A. Fawky, M. Khaliel, A. El-Awamry, M. El-Hadidy and T. Kaiser, "Novel Pseudo-Noise coded chipless RFID system for clutter removal and tag detection," IEEE International Conference on RFID (RFID), San Diego, CA, 2015, pp. 100-104, doi: 10.1109/RFID.2015.7113079.

8. J. G. D. Hester and M. M. Tentzeris, "Inkjet-Printed Flexible mm-Wave Van-Atta Reflectarrays: A Solution for Ultralong-Range Dense Multitag and Multisensing Chipless RFID Implementations for IoT Smart Skins," in *IEEE Transactions on Microwave Theory and Techniques*, vol. 64, no. 12, pp. 4763-4773, Dec. 2016. doi: 10.1109/TMTT.2016.2623790.

9. J. Wenger, "Automotive radar - status and perspectives," IEEE Compound Semiconductor Integrated Circuit Symposium, 2005. CSIC '05., Palm Springs, CA, USA, 2005, pp. 4, doi: 10.1109/CSICS.2005.1531741.

10. https://altairhyperworks.com/product/FEKO

11. https://zmt.swiss/sim4life/